Oxidation Study of Pure Tin and Its Alloys via Electrochemical Reduction Analysis

SUNGIL CHO,[1,3] JIN YU,[1] SUNG K. KANG,[2] and DA-YUAN SHIH[2]

1.—Department of Materials Science and Engineering, Korea Advanced Institute of Science and Technology (KAIST), Daejon 305-701, Republic of Korea. 2.—IBM, T. J. Watson Research Center, Yorktown Heights, NY 10598. 3.—E-mail: sicho@kaist.ac.kr

The oxidation of pure Sn and high Pb-Sn alloys was investigated under different oxidizing conditions of temperature and humidity. Both the chemical nature and the amount of oxides were characterized using electrochemical reduction analysis by measuring the electrolytic reduction potential and total transferred electrical charges. For pure tin, SnO grew faster under humid conditions than in dry air. A very thin (<10 Å) layer of SnO_2 was formed on the top surface under humid conditions. The mixture of SnO and SnO_2 was found for oxidation at 150°C. For oxidation of high Pb-Sn alloys, tin was preferentially oxidized on the surface, and tin content over the solubility limit suppressed the formation of lead oxide. For the evaporated Pb-3Sn alloy reflowed two times at 370°C under H_2 atmosphere, tin was enriched on the surface as tin dendrites and lead oxide was formed in the tin-depleted region that surrounds tin dendrites.

Key words: Oxidation, solder, Sn alloys, electrochemical reduction analysis

INTRODUCTION

Most metal tends to form surface oxides spontaneously under ambient or aqueous condition.[1,2] The presence of oxides on the surface of solder alloys used in microelectronics applications is of critical importance. It affects the formation of an otherwise good solder joint by degrading its wettability and solderability.[3,4] In manufacturing, a flux material is typically used to reduce surface oxides and to protect the joining surfaces from further oxidation during reflow at elevated temperatures. However, the environmentally friendly flux materials used in microelectronics assembly such as no-clean flux and water-soluble flux do not guarantee an oxide-free surface during soldering.[5]

Continued interaction of oxygen with solder during the service period of microelectronics products can affect the mechanical reliability of solder joints. It was reported that when a Pb-rich Sn solder is fatigued in air, the intergranular cracks dominate; however, when it is fatigued in a vacuum, the transgranular cracks dominate. The fatigue life is also shortened for the air-fatigued samples, suggesting that oxygen diffusion at grain boundaries plays an important role in the lifetime of solder joints.[6] Hence, it is important to characterize the oxidation behavior of solder joints during the soldering process as well as in service to better understand their reliability issues.

Considering Gibbs free energies in Table I, the formation of tin oxides is thermodynamically favored in the Sn-Pb system so that it is expected that tin oxide would be formed preferentially. Tin hydroxides, $Sn(OH)_2$ and $Sn(OH)_4$, can also form preferentially based on the Gibbs free energy consideration, but the hydroxides are unstable with respect to the corresponding oxides and would not form under ambient conditions or may undergo dehydration.[9]

Preferential oxidation of tin in the Sn-Pb system has been reported. Bird[10] and Farrell[11] have found that surface enrichment of tin in lead-tin alloy using x-ray photoelectron spectroscopy (XPS). Konetzki and Chang[12] found that tin was preferentially oxidized on the surface of Sn-Pb alloys containing only 2.9at%Sn. Bevolo et al.[13] and Shah and Eurof Davies[14] showed that SnO_2 was enriched at the outer surface and the surface was completely covered with a SnO_2 layer in the laboratory environment. High-lead alloy such as

(Received September 13, 2004; accepted November 8, 2004)

Table I. Standard Gibbs Free Energies,[7] Equilibrium Reduction Potentials, and Measured Reduction Potentials of Cu, Pb, and Sn Oxides

Oxide	Free Energy of Formation, ΔG° (298K, kJ/mole)	Equilibrium Potential (V)	Measured Potential (V)
Cu_2O	−292.9[8]	−0.267	−0.625
CuO	−254.6[8]	−0.168	−0.406
PbO	−187.9	−0.4639	−0.554
SnO	−251.9	−0.7955	−0.972
SnO_2	−515.8	−0.8266	−1.10
$Sn(OH)_2$	−491.6[12]	−0.8090	—

Pb-3at.%Sn has been shown to exhibit surface segregation of tin, especially in the presence of oxygen.[15] Tin was found to be highly segregated around grain boundaries. The rate of surface segregation of tin was considerably enhanced by exposing the clean surface to oxygen, which indicates that the oxidation of tin could be the driving force of tin diffusion to the surface along grain boundaries.

ELECTROCHEMICAL REDUCTION ANALYSIS

There are many techniques[1] to characterize the surface oxides. The Auger electron spectroscopy (AES),[16] XPS,[11] low energy electron loss spectroscopy (LEELS),[13] and Mössbauer[17] techniques are for chemical information of oxides. Ellipsometry, x-ray emission, gravimetric method, and AES are techniques to measure oxide thickness. None of these techniques provides complete information of the oxides. Electrochemical reduction analysis is known to be an inexpensive, simple, and yet relatively precise technique to measure quantitatively both the type and the thickness of oxides formed on metal surfaces.[4] In this study, a SurfaceScan QC-100 tool developed by ECI Technology (East Rutherford, NJ) for electrochemical reduction analysis was used to study the oxidation of pure Sn and high Pb-Sn solder alloys.

The surface to be analyzed is brought in contact with a borate buffer solution (9.55 g/L sodium borate and 6.18 g/L boric acid).[18] A constant cathodic current is applied between the surface and an inert counter electrode.[4] The change of cathode potential of the oxidized surface during reduction is recorded as a function of time relative to a reference electrode. The recorded potential-time curve consists of a series of potential durations (plateaus), which is characteristic of each type of oxides reduced. The equilibrium reduction potentials for Sn and Pb oxides are shown in Table I. After completing the reduction process, the final plateau of hydrogen evolution begins due to reduction of the electrolyte.

Equilibrium reduction potentials of oxides can be calculated from thermodynamic stability data using the Nernst equation[2]:

$$E = E^\circ - \frac{0.0591}{n} pH \quad (1)$$

$$E^\circ = \frac{\sum \nu \Delta G^\circ}{nF} \quad (2)$$

Equations 1 and 2 are the relations between electrode reactions in aqueous solutions and Gibbs free energy at 298 K. The term E is equilibrium potential, E° is standard equilibrium potential, n is the number of electrons used for reaction, ν is stoichiometric coefficient of reaction, and F is the Faraday constant. Equation 1 is represented in a graphical form on the Pourbaix diagram, which shows the equilibrium potentials according to the pH of solutions. Table I shows the Gibbs free energy,[7,9] ΔG°, of each oxide and equilibrium reduction potentials calculated from the Nernst Eq. 1 using ΔG° values according to the reaction typified by[4]

$$SnO + 2H^+ + 2e^- = Sn + H_2O \quad (3)$$

All the potentials calculated are expressed against the standard Ag/AgCl electrode (E = 10.2224 versus SHE (standard hydrogen electrode))[17] in a solution of pH 8.4.

The thickness of oxide can be calculated using the modified Faraday's equation,[20] where the time required to reduce surface oxide is directly proportional to the thickness of an oxide and the oxide is assumed in the form of a uniform layer:

$$T = (Mit) / (nFSD) \quad (4)$$

where M is molecular weight, i is current, t is time, n is the number of electrons, F is the Faraday's constant, D is the density of a coating, and S is surface area.

EXPERIMENTAL PROCEDURE

All electrochemical experiments were performed in nitrogen-saturated pH 8.4 borate buffer solution (9.55 g/L sodium borate and 6.18 g/L boric acid), which provides minimal solubility for tin oxides using Ag/AgCl as a reference electrode (+0.2224 versus SHE).[4,14,19] The current density used for electrochemical reduction analysis should be optimized to provide good resolution, accuracy, and a short analysis time.[4] To find an optimal current density value for oxide reduction analysis, the electrochemical reduction of evaporated Pb-3Sn reflowed at 370°C was performed at various current densities.

High-purity oxide powder (PbO, SnO, SnO_2, Cu_2O, CuO) was pressed onto a pure tin foil and electrochemically reduced at –20 μA/cm^2 to obtain an actual reduction potential of each oxide. This was used as a standard to calibrate and distinguish different types

of oxides formed on various tin alloys. The measured reduction potentials of each oxide were compared with the equilibrium values. A powder mixture, (PbO + SnO) and (SnO + SnO_2), was also prepared to investigate any reduction potential changes and to identify individual oxides in the reduction curve.

After completing the reduction process of oxides, the final plateau of hydrogen evolution begins due to the reduction of the electrolyte. The surface of pure Cu, Sn, Pb, Au, and eutectic Sn-Pb was reduced to obtain hydrogen evolution potentials.

Pure tin and high Pb-Sn alloy (Pb-1, 2, 2.5, 3, 3.5wt.%Sn) foils (100-μm thick, Indium Corporation of America) were cut to 25 mm × 10 mm. The surface of test samples was fully reduced electrochemically using the same electrolyte used for the reduction analysis (pH 8.4 borate buffer solution) at a high current density before being placed in an oxidizing furnace. Samples were thermally oxidized in a furnace at 85°C, 150°C, and T/H (85°C, 85% relative humidity) conditions. Oxides formed on the surface of samples were electrochemically reduced at -20 μA/cm^2 to obtain potential versus time curves.

Pb-3Sn alloy (25 μm) was evaporated on a silicon wafer with a thin film structure of Cr(150 nm)/CrCu(100 nm)/Cu(1100 nm)/Au(100 nm). The Si wafer was then reflowed two times at 370°C under H_2 atmosphere. Samples cut from the wafer were thermally oxidized in a furnace at 150°C, 200°C, 250°C, and T/H (85°C, 85% RH) conditions. Oxides formed on the surface of samples were electrochemically reduced at -30 μA/cm^2.

The AES and XPS or ESCA were applied to surface analysis of oxides. Auger analysis was carried out on a PHI model 4300 (Perkin-Elmer, Boston, MA) operated at 2×10^{-7} Torr. Primary electron beam energy of 5 keV and 300 nA was used. An argon ion gun with a voltage of 3 keV and 15 mA (current density = 120 μAcm^{-2}) was employed for depth profiling. The XPS data were obtained using a ESCA2000 (VG Microtech, Waltham, MA) which was equipped with a Mg source (MgK_α). The pressure in the analyzer chamber was maintained at less than 10^{-7} Torr during analysis. The Mg x-ray beam was operated at 12 kV and 15 mA.

RESULTS AND DISCUSSION

Current Density Effects

The current density used for electrochemical reduction analysis should be optimal for good resolution, accuracy, and a short analysis time.[4] Figure 1 shows the reduction curves obtained from same samples at different current densities. Table II shows the oxide thicknesses calculated from Fig. 1 using Eq. 4. It shows that the oxide thicknesses of the same samples are different depending on current densities. As the current density increases, the reduction potential tends to shift toward a more negative voltage and to become less distinctive because reduction processes deviate further from equilibrium. Therefore, the amount of oxide measured is smaller than that measured at low current densities. On the other hand, at low current densities, the oxide thickness was overestimated due to the contribution from the reduction of residual oxygen and impurities that might cause the measured oxide amount being larger.[4] In general, the magnitude of applied current density is chosen to avoid excessive polarization of the cathode and is typically under –100 μA/cm^2.[4] As a result, the optimal current density range is found to be -30 μA/cm^2 to –260 μA/cm^2, where the oxide thickness calculated remains almost constant, which is in good agreement with the previous observations.[4]

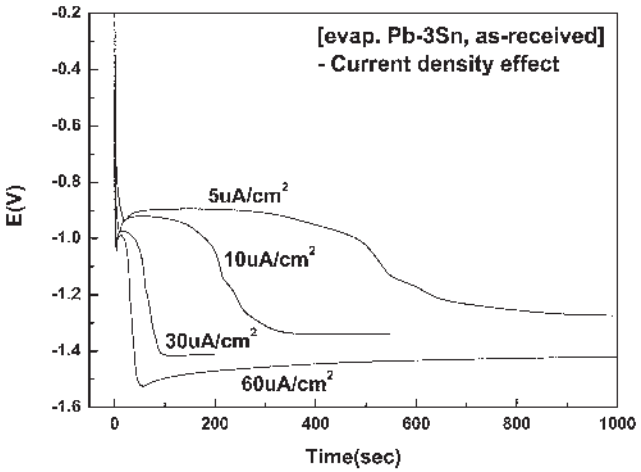

Fig. 1. Current density effects: reduction curves at various current densities for the same sample.

Table II. Current Density Effects: Oxide Thicknesses Measured at Various Current Densities for the Same Samples

CD (μA/cm^2)	Thickness (Å)
−5	28(SnO) + 9(SnO_2) = 37
−10	22(SnO) + 6(SnO_2) = 28
−30	18(SnO) + 5(SnO_2) = 23
−60	17(SnO) + 4(SnO_2) = 21

Reduction Potential of Oxide Powders

Figure 2 shows the reduction curves for pure oxide powders of Sn, Pb, and Cu and they were used as a standard to calibrate and distinguish different types of oxides in this study. The measured reduction potential of each oxide is listed in Table I to compare with the equilibrium values. Because of kinetic factors, actual reduction potentials are generally more negative than theoretical values in agreement with the previous observation.[4] Although the equilibrium potential of SnO_2 is almost the same as SnO, the measured potential for SnO_2 is somewhat lower than that of SnO, indicating that the reduction of SnO_2 is more kinetically inhibited than SnO. Owing to this situation, SnO_2 can be resolved from SnO in the reduction curve.

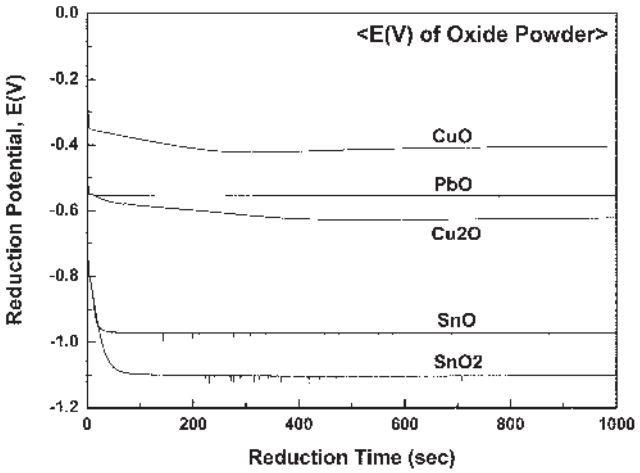

Fig. 2. Reduction potentials measured for pure oxide powders.

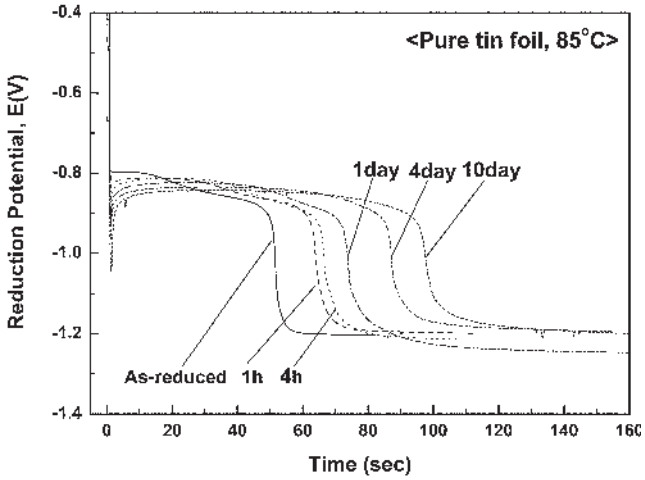

Fig. 3. Reduction curves for pure tin oxidized at 85°C in dry air for several times.

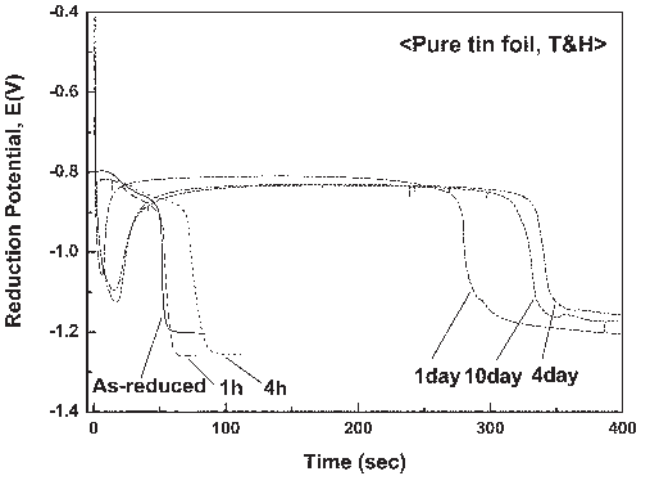

Fig. 4. Reduction curves for pure tin oxidized at T/H for several times.

Hydrogen Evolution Potential

After completing the reduction process, the final plateau of hydrogen evolution begins due to the reduction of the electrolyte. Oxides requiring more negative potentials for reduction than hydrogen evolution potential may not be reduced before the onset of hydrogen evolution. Thermodynamical reduction potential of hydrogen evolution is −0.72 (versus Ag/AgCl) in pH 8.4 solution,[4] and this is positive enough to cause errors in measuring the amount of Sn oxides. Fortunately, most metals are not very effective proton reduction catalysts so that hydrogen evolution on their surfaces requires additional negative voltage (overvoltage), which extends the voltage range available for oxide reduction.[4] Table III shows the steady-state hydrogen evolution potentials measured at $-20\ \mu A/cm^2$ in pH 8.4 borate buffer solutions for various metals. As can be seen in Tables I and III, oxide reduction potentials are higher than the hydrogen evolution potentials so that most oxide species of tin, lead, eutectic tin-lead, and copper can be fully reduced on their surfaces. It is expected that surface roughness, grain structure, and alloying ratio could affect the oxide reduction potentials by affecting the actual current density and kinetic factors.[4]

Oxidation of Pure Tin

Figures 3–5 show the growth of tin oxides on pure tin surface at 85°C, T/H, and 150°C, respectively. The native oxide of pure Sn formed in air right after reduction (i.e., as-reduced) was SnO and the thickness was about 10 Å. The SnO was formed at 85°C and the T/H condition with the reduction potential of about −0.8 V, which is close to the equilibrium value. As oxidation time increases, the reduction potential of SnO tends to shift toward negative voltage. SnO grows faster under the humid condition than in dry air. A small negative peak at the initial stage of reduction for a long time aging (>1 day) in Fig. 4 is thought to be the reduction peak of a very thin SnO_2 overlayer.[4,14] Since SnO reduces first at a more positive potential with respect to SnO_2, the initial peak indicates that SnO_2 exists in the form of an overlayer preventing the exposure of SnO to the electrolyte. The small negative peak around the reduction potential of SnO_2 increases in thickness as the oxidation time increases under the T/H condition.

Figure 5 shows that SnO grows up to 4 h at 150°C and shrinks a little up to 12 h, which indicates that a part of SnO transforms to SnO_2, and then SnO_2 begins to grow after 12 h. The reduction curve of 12 h aging clearly shows two potential plateaus in

Table III. Hydrogen Evolution Potentials (versus Ag/AgCl) for Various Metals in Borate Buffer Solution (pH 8.4) at $-20\ \mu Acm^{-2}$

Metal	Published[4] (V)	Experiment (V)
Copper	−1.03	−1.04
Eutectic Sn-Pb	−1.23	−1.39
Tin	−1.25	−1.22
Lead	−1.33	−1.36
Gold	−0.88	−0.97

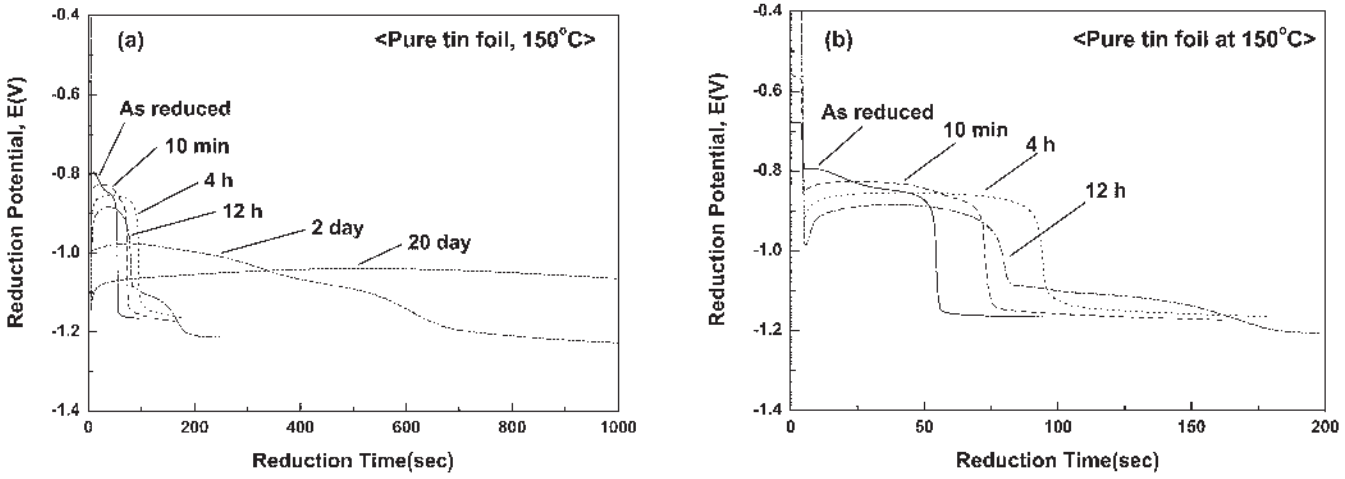

Fig. 5. (a) Reduction curves for pure tin oxidized at 150°C and (b) magnification of (a) for short time aging.

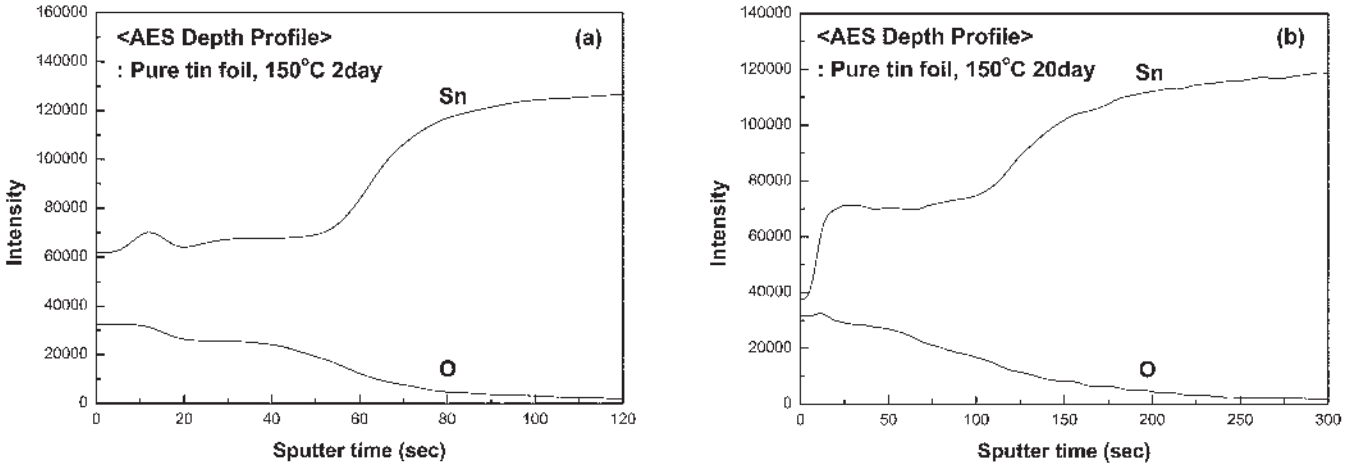

Fig. 6. AES depth profile of pure tin foil oxidized at 150°C for (a) 2 days and (b) 20 days.

Fig. 5b, the more positive one is SnO and the more negative one is SnO_2. As oxidation time increases, the reduction potential of SnO tends to shift toward negative voltage. The reduction curve does not show a clear distinction between SnO and SnO_2 for prolonged aging times. For 20-day oxidation, reduction potential starts at about −1.1V and therefore it seems to consist of SnO_2 at the outer surface region. This was verified by AES and XPS analysis. The AES depth profiling in Fig. 6 shows the enrichment of oxygen at the outer surface of 20-day aging in comparison with 2-day aging.

Figure 7 shows XPS spectra of pure tin foil oxidized at 150°C. The spectra were analyzed using PC software "XPSPEAK" and a peak separation was performed for the spectrum of the as-reduced samples. Tin has three different chemical states, pure metal and two oxidation states, and in principle the chemical shift should differ for each state. Farrell[11] had obtained the binding energies of tin 3d from tin and its oxides using pure metal and oxide powders, which is represented in Table IV. From Fig. 7, it is clear that one metallic and two oxidation states of tin can be differentiated owing to the chemical shift. The binding

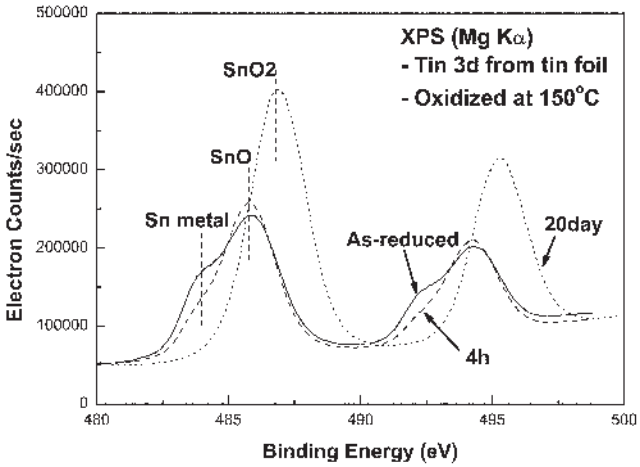

Fig. 7. XPS spectra of pure tin foil oxidized at 150°C for several times. The as-reduced spectrum shows a metallic Sn peak at 484.0 eV by peak separation.

energy of tin 3d was tabulated in Table IV, which is in good agreement with the result of Farrell. The spectrum of the as-reduced sample in Fig. 7 shows the pure tin peak at 484.0 eV. The depth resolution of

Table IV. Binding Energies of Tin $3d_{5/2}$ from Tin and Its Oxides

Tin 3d	Farrell[11] (eV)	Experiment (eV)
Tin metal	484.2	484.0
SnO	485.9	485.9 (±0.15)
SnO2	486.8	486.7 (±0.23)

XPS for metal[10] is about 20 Å, and therefore, the detection of pure tin peak indicates that the thickness of native oxide is less than 20 Å, which is in good agreement with the value (~10 Å) obtained from reduction analysis using Eq. 4.

Oxidation of High Pb-Sn

Figure 8 shows surface oxides formed on pure lead and high Pb-Sn alloys (Pb-1, 2, 2.5, 3, 3.5wt.%Sn), which had been stored at room temperature for 18 years. One can see a dramatic decrease of lead oxide, PbO, as tin content increases, especially over room-temperature solubility limit of tin (~1.8 wt.%) in lead. The thickness of PbO was about 700 Å for pure lead and 30 Å for Pb-1Sn. Pb-1Sn shows SnO and SnO_2 as well as PbO. Only tin oxide could be seen on 2–3.5wt.%Sn and the thickness was very thin (<20 Å), which indicates that the tin content of over solubility limit can effectively suppress the formation of lead oxide. Figure 9 also shows the tin content effects on the formation of lead oxide on Pb-3Sn alloys. The surface of Pb-3Sn foil was electrochemically reduced to remove surface oxides and then oxidized at 85°C for 1 h. The reduction curve of as-reduced sample clearly shows two plateaus of PbO and SnO. After oxidation of just 1 h at 85°C, lead oxide shrank and only tin oxide could be found, which indicates that tin is a very surface-active element and preferentially oxidized. The preferential oxidation of tin in the near-surface region of high Pb-Sn alloy (2.9at.%Sn) has been reported by Konetzki and Chang[12] using AES surface analysis. Opila[15] has shown that tin was highly segregated around grain boundaries in Pb-3at.%Sn, which indicates that the grain boundary is a fast diffusion path of tin and oxygen for oxidation. Bird[10] and Farrell[11] have also found surface enrichment of tin in lead-tin alloy using XPS.

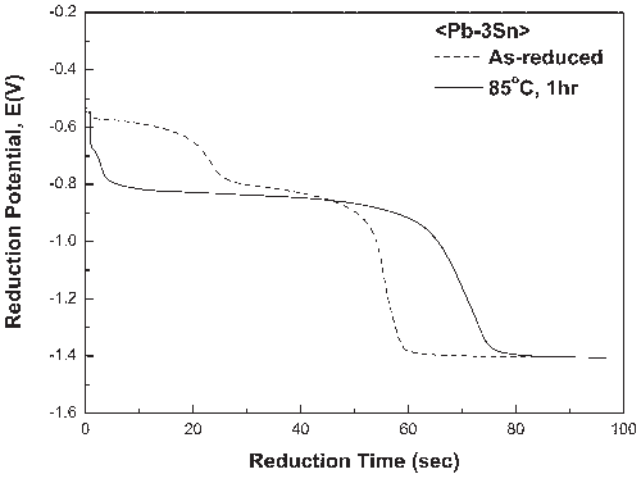

Fig. 9. Reduction curve of as-reduced Pb-3Sn foil oxidized at 85°C for 1 h, which shows the shrink of lead oxide, PbO.

Figure 10 shows surface oxides on the evaporated Pb-3Sn, which was reflowed two times at 370°C under H_2 atmosphere. Almost all area of evaporated Pb-3Sn exhibits gray color, as shown in Fig. 10a, but some area shows blue stains, as in Fig. 10b. From the oxide reduction curves for each area given in Fig. 11, the blue color stains surrounding the dendrites were found to be lead oxide, PbO. To support this result, electron microprobe analyzer (EMPA) dot mapping was performed for the blue stain area in Fig. 11. In each mapping of lead, tin, and oxygen, bright contrast means a large signal of the element. The tin mapping shows that dendrites are made of tin, which was severely segregated on the surface. The bright area of the oxygen map matches well with the

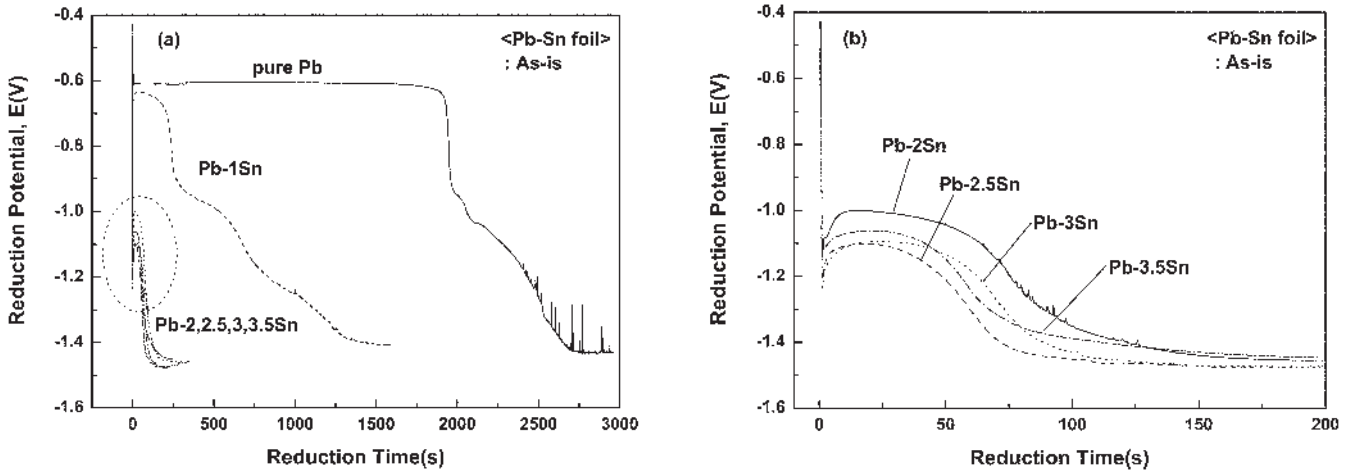

Fig. 8. (a) Reduction curves of high Pb-Sn alloys showing the shrink of PbO and (b) magnification of high Pb-Sn with tin content over solubility limit (≥2wt.%Sn).

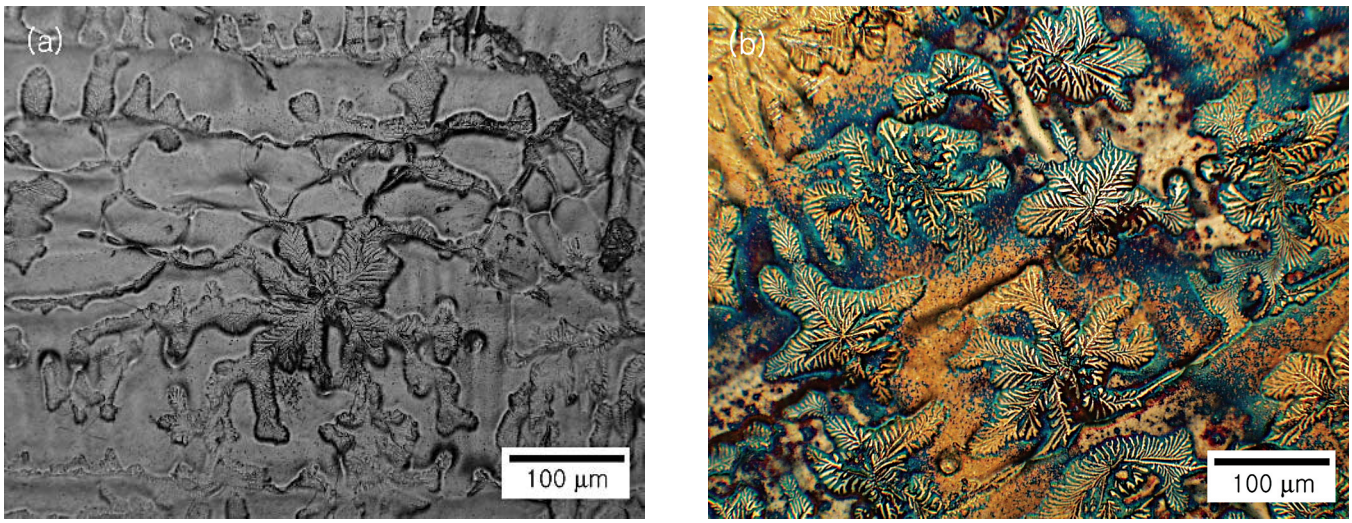

Fig. 10. Optical images of surface of evaporated Pb-3Sn reflowed two times at 370°C under H_2 atmosphere: (a) a monotone surface and (b) blue stains around tin dendrites.

lead-rich area, and it surrounds tin dendrite precipitates, which indicates that lead oxide was formed in the tin-depleted region around tin dendrites.

SUMMARY

The electrochemical reduction analysis method has been successfully applied to obtain the information on both the nature of oxide and oxide thicknesses formed on pure Sn and high Pb-Sn solder under different oxidizing conditions. Other surface analytical methods such as AES and XPS were also employed to supplement the results from the electrochemical analysis of oxides. Several important results are summarized as follows.

- For oxidation of pure tin, the oxide formed at 85°C and T/H (85°C, 85% R.H.) was SnO and it grew faster under the humid condition than in dry air. Under humid condition, the surface of tin was covered with a blocking layer of SnO_2 over SnO. During the oxidation of pure Sn at 150°C, SnO forms first on the tin surface and then SnO_2 grows during long aging. The mixture of SnO and SnO_2 was also confirmed by the analysis of reduction and AES.
- For oxidation of high Pb-Sn alloys, tin is preferentially oxidized on the surface. The tin content above the solubility limit in lead (~1.8 wt.% at room temperature) can effectively suppress the formation of lead oxide. In the oxidation of evaporated Pb-3Sn alloy (reflowed two times at 370°C under H_2 atmosphere), tin was precipitated on the surface as tin dendrites. Blue-colored lead oxide was formed in the tin-depleted region surrounding tin dendrites.

Further investigation is in progress with Sn-rich, Pb-free solders with various alloying contents to understand their oxidation behaviors and mechanisms and thereby alleviate any reliability concerns associated with them.

ACKNOWLEDGEMENTS

This work was supported by the Center for Electronic Packaging Materials, Korea Science and Engineering Foundation. One of the authors (SC) was a visiting graduate student at IBM, T.J. Watson Research Center, under the KAIST-IBM joint study program. The authors thank Dr. Donald W. Henderson for providing the reduction equipment and discussing the experimental results in the early stage of the investigation. They also thank A. Wirsing for providing evaporated Pb-Sn solder samples and Donovan Leonard for performing EMPA with oxidized samples.

REFERENCES

1. A.T. Fromhold, Jr., *Theory of Metal Oxidation, Vol. 1 Fundamentals* (New York: North-Holland Publishing Company, 1976), pp. 3–49.
2. Marcel Pourbaix, *Atlas of Electrochemical Equilibria in Aqueous Solutions* (New York: Pergamon Press, 1966), pp. 31–50.
3. Frederick G. Yost, F. Michael Hosking, and Darrel R. Frear, *The Mechanics of Solder Alloy, Wetting & Spreading* (New York: Van Nostrand Reinhold, 1993), pp. 155–189.
4. D. Morgan Tench, D.P. Anderson, and P. Kim, *J. Appl. Electrochem.* 24, 18 (1994).
5. Rao R. Tummala et al., *Fundamentals of Microsystems Packaging* (New York: McGraw-Hill, 2001), pp. 672–693.
6. D.A. Sluzewski, Y.A. Chang, and V.C. Marcotte: *Mater. Res. Soc. Symp. Proc.* 167, 353 (1990).
7. David R. Lide, *Handbook of Chemistry and Physics*, 73rd ed. (Boca Raton, FL: CRC Press, 1993), pp. 5–75.
8. Frederick G. Yost et al., *The Mechanics of Solder Alloy "Wetting & Spreading"* (New York: Van Nostrand Reinhold, 1993), pp. 155–189.
9. C.I. House and G.H. Kelsall, *Electrochim. Acta* 29, 1459 (1984).
10. R.J. Bird, *J. Met. Sci.* 7, 109 (1973).
11. T. Farrell, *Met. Sci.* 10, 87 (1976).
12. R.A. Konetzki and Y.A. Chang, *J. Mater. Res.* 3, 466 (1988).
13. A.J. Bevolo, J.D. Verhoeven, and M. Noack, *Surf. Sci.* 134, 499 (1983).
14. S.N. Shah and D. Eurof Davies: *Electrochim. Acta* 8, 663 (1963).

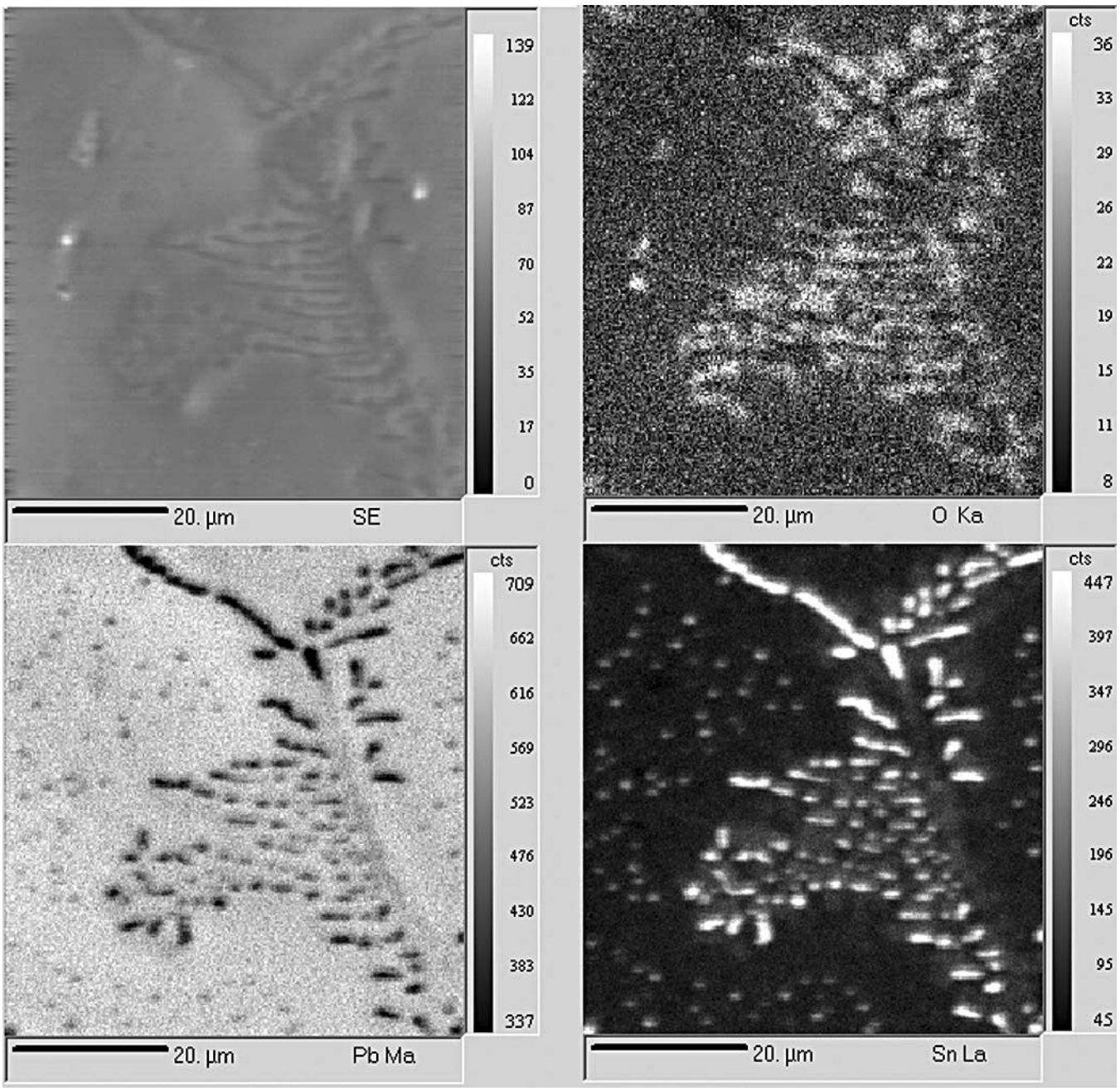

Fig. 11. EPMA dot mapping of blue stained surface of evaporated Pb-3Sn, which was reflowed two times at 370°C under H_2 atmosphere.

15. R.L. Opila, *J. Vac. Sci. Technol.* A 4, 173 (1986).
16. E.E. de Kluizenaar, *J. Vac. Sci. Technol.* A 1, 1480 (1983).
17. M.L. Varsányi, J. Jaén, A. Vértes, and L. Kiss, *Electrochim. Acta* 30, 529 (1985).
18. D.M. Tench and D.P. Anderson, U.S. patent 5,262,022 (19 Nov. 1993).
19. S.E.S. El Wakkad, A.M. Shams Dl Din, and Jeannette A. El Sayed, *J. Chem. Soc. London,* 3103 (1954).
20. Peter Bratin, Michael Pavlov, and Gene Chalyt, "Surface Evaluation of the Immersion Tin Coatings via Sequential Electrochemical Reduction Analysis (SERA)," Research Report from Homepage of ECI technology (www.ecitechnology.com).